7-2017

Metabolite profiling of infection-associated metabolic markers of onchocerciasis.

Sasisekhar Bennuru
NIH

Sara Lustigman
New York Blood Center

David Abraham
Thomas Jefferson University

Thomas B. Nutman
NIH

Published in final edited form as:

Mol Biochem Parasitol. 2017 July ; 215: 58–69. doi:10.1016/j.molbiopara.2017.01.008.

Metabolite profiling of infection-associated metabolic markers of onchocerciasis

Sasisekhar Bennuru[1], **Sara Lustigman**[2], **David Abraham**[3], and **Thomas B Nutman**[1]

[1]Laboratory of Parasitic Diseases, NIAID, NIH, Bethesda, MD, USA

[2]New York Blood Center, New York, NY, USA

[3]Thomas Jefferson University, Philadelphia, PA, USA

Abstract

The global efforts for onchocerciasis elimination may require additional tools (safe micro and macrofilaricidal drugs, vaccines and biomarkers) as elimination efforts move toward the “end game”. Efforts toward the identification of suitable biomarkers have focused on specific protein(s) and/or nucleic acids, but metabolites present an alternative option as they have limited half-lives and are the result of combinatorial effects. In comparison to previously used methodology of LCMS for metabolomic approaches, we used a non-targeted capillary electrophoresis time-of-flight mass spectrometry (CE-TOFMS) to analyze the serum metabolic profiles of *Ov*-infected and - uninfected individuals (n=20). We identified 286 known metabolites (167 in the cation mode and 119 in the anion mode). In addition, putative metabolites were identified based on KEGG (51), HMDB (37) and HMT (6) databases. One hundred ten of these putative metabolites were quantified based on peak areas of internal standards and their ability to be mapped to known pathways (primary-, carbon-, lipid-, amino acid-, nucleotide and coenzyme-metabolism). Multivariate analysis demonstrated clustering and segregation of some of these metabolites to either the infected or control groups. The levels of serotonin, hypoxanthine, pipecolic acid and inosine were significantly elevated in those with onchocerciasis, whereas the levels of glycerophosphocholine, choline and adenine were significantly lower. This non-targeted metabolomic approach provides a global view of the metabolic variations that occur during *Ov* infection and thus allow the discovery of key metabolites (and associated pathways) that may serve as useful biomarkers in human onchocerciasis.

Keywords

Onchocerca volvulus; metabolome; biomarker

Corresponding author: Sasisekhar Bennuru; bennurus@niaid.nih.gov.

Introduction

Onchocerciasis or 'river blindness' is a neglected tropical disease (NTD) that is caused by a parasitic nematode, *Onchocerca volvulus* (Ov). Successful mass drug administration (MDA) programs in the Americas and small parts of Africa now presage the possibility of elimination of the disease [1, 2]. Successful intervention relies on surveillance programs for assessing the recrudescence of infection, which, in turn, depends on additional tools (safe micro and macrofilaricidal drugs, vaccines and biomarkers [3, 4]). Among these potential tools, one that has gained traction, of late, is a biomarker(s) that would identify the presence of living adult worms. Serological approaches, although useful in many settings, are unable to distinguish a past infection from an ongoing infection in that antibody responses persist despite appropriate therapy. Although the identification of parasite-specific circulating protein(s) and/or DNA has been quite useful they may not be adequate for elimination programs (reviewed in [5]). Metabolomics may provide an alternate strategy, because metabolites have very limited half-lives and because they are the result of combinatorial effects of the genome, the transcriptome, the proteome and the environment. However, metabolomic analyses are complicated by the continuous and dynamic changes of the metabolites, small intermediates, or end products of enzyme-catalyzed biochemical reactions. This is further complicated in onchocerciasis, as humans are the only definitive host and there are no existing immunocompetent small animal models for propagating the life cycle. *Onchocerca ochengi*, a natural filarial parasite of cattle is the closest related nematode and is often used as a surrogate for *Ov* infections.

Traditionally, diagnosis of onchocerciasis relied on positivity for microfilariae from skin snips [6], PCR for the interspersed O-150 repeat [7] or IgG4 responses to Ov16 [8-12]. Recent modeling studies indicate the usefulness of Ov16 seropositivity in conjunction with skin snip results for MDA and surveillance programs for onchocerciasis [13]. A search for better biomarkers resulted in the identification of parasite-derived microRNAs [14, 15] or seropositivity with novel stage-specific proteins [16] though robust assays to detect these in low quantity in human specimens have not been developed. Moreover, whether any of these biomarkers provide the necessary sensitivity, specificity and dynamic range for use in endemic areas remains to be seen. Another promising approach was the LC-MS based metabolomics analysis of serum [17] or urine [18] of Ov-infected individuals. Though the latter study identified N-acetyltyramine-O,β- glucuronide (NATOG) as a potential unique marker for onchocerciasis in humans [17, 18] and shown to be detectable before the onset of microfilariae in jirds infected with *L. sigmodontis* [19], its applicability has been questioned as the presence of NATOG failed to differentiate nodulepositive but amicrofilaraemic individuals from control groups [20].

Metabolomic studies for detecting and quantifying multiple small chemical metabolites of complex biological samples have relied on analytical platforms such as nuclear magnetic resonance (NMR), gas or liquid chromatography coupled to mass spectrometry (GC-MS/LC-MS) and capillary electrophoresis coupled to mass spectrometry (CE-MS). We utilized capillary electrophoresis time-of-flight mass spectroscopy (CE-TOFMS) - a relatively new mass spectrometry method that can measure metabolites of higher ionization and lower molecular weight in onchocerciasis infected and uninfected control sera. This

non-targeted metabolomic approach provides a global view of the metabolic variations that occur during infection and allowed for the discovery of key metabolites that can discriminate *Ov*-infected individuals from uninfected-individuals.

Materials and Methods

Patient samples

The human plasma samples from *Ov* infected (n=10) were from regions of Ecuador and Guatemala and were obtained using protocols approved by the IRB (OH86-I-0029) of the National Institute of Allergy and Infectious Diseases. The samples were archived plasma collected prior to implementation of mass drug administration programs and positive by skin snip microfilariae (mf) (50-95 mf). The uninfected donor plasma came from healthy volunteers (n=10) from the NIH blood bank.

Sample processing

The plasma samples were processed and analyzed at Human Metabolome Technologies (HMT, Yamagata, Japan). Briefly, 50 μl of sample was mixed with 450 μl of methanol containing internal standards (10 μM). Chloroform (500 μl) and Milli-Q water (200 μl) were added next, mixed thoroughly and centrifuged at 2,300 × g at 4°C for 5 mins. The aqueous layer (~400 μl) was filtered through a 5-kDa cut-off filter to remove macromolecules. The filtrate was concentrated and resuspended in 25 μl of ultrapure water immediately before measurement.

Measurement of metabolites

Serum metabolic profiling was analyzed using a capillary electrophoresis time-of-flight mass spectrometry (CE-TOFMS) system (Agilent 6210 TOF, Agilent Technologies, USA) in cationic and anionic modes) as described previously [21], with a mass range of 50 to 1200 and mass accuracy of <2 ppm and capability to resolve and quantitate isomers. Cationic metabolites were analyzed using a fused silica capillary (50 μm × 80cm) with Cation Buffer Solution (H3301-1001, HMT) as the electrolyte. The sample was injected at a pressure of 50 mbar for 10 sec. The applied voltage was set to 27 kV. Electrospray ionization-mass spectrometry (ESI-MS) was conducted in the positive ion mode and the capillary voltage was set to 4,000 V. Anionic metabolites were analyzed using a fused silica capillary (50 μm × 80cm) with Anion Buffer Solution (H3302-1023, HMT) as the electrolyte. The sample was injected at a pressure of 50 mbar for 25 sec. The applied voltage was set to 30 kV. ESI-MS was conducted in the negative ion mode and the capillary voltage was set to 3,500 V. Exact mass data from the cationic and anionic modes were acquired over a 50 to1,000 m/z range. The samples were diluted 2-fold and 5-fold for the measurement in cation and anion modes respectively to improve the quality of CE-MS analysis.

Data Processing and Analysis

Peaks detected in CE-TOFMS analysis were extracted (that excludes peaks present in only a few samples, solvent and salt adduct-derived and isotope peaks) using automatic integration software (MasterHands ver 2.16.0.15 developed at Keio University) to obtain peak

information including *m/z*, migration time (MT) and peak area. The peak area was converted to relative peak area, where

$$Relative\ Peak\ Area = \frac{Metabolite\ Peak\ Area}{Internal\ Standard\ Peak\ Area}$$

Putative metabolites were assigned from HMTs standard library and known and unknown peak library on the basis of *m/z* and MT. In addition, putative metabolites were also assigned from KEGG database [22], HMDB database [23] and HMT peptide list on the basis of theoretical m/z calculated from the molecular formula. The tolerance was ±0.5 min in MT and ±10 ppm in *m/z* where:

$$Mass\ Error = \frac{Measured\ Value - Theoretical\ Value}{Measured\ Value} \times 10^6$$

Absolute quantification was performed for 110 metabolites including glycolytic and TCA cycle intermediates, amino acids and nucleic acids. All metabolite concentrations were calculated by normalizing the peak area of each metabolite with respect to the area of each metabolite with respect to the area of the internal standards. The internal standards used for relative peak area were 3-aminopiperzine, methionine sulfone, N,N-diethylphenylacetamide for cationic mode; and camphor-10-sulfonic acid, naphthol-4,8-disulfonic acid, Trimesic acid for anionic mode, while absolute quantification (in μM) of metabolites were performed by using single-point (100 μM) calibrations.

Statistical Analyses

Analysis of the data was performed using PeakStat v 3.18; SampleStat v3.14 (in-house software at HMT) or JMP (SAS, Inc). Data distribution and discriminatory metabolomic profiles by multivariate analyses using principal component analysis (PCA) and partial least squares discriminant analysis (PLS-DA) were performed using JMP and Metaboanalyst [24]. Statistical analyses for normalization, logarithmic transformation and data scaling were also performed using MetaboAnalyst to identify differentially expressed metabolites. On the basis of the variable importance in projection (VIP) threshold of 1 (VIP≥1), and Empirical Bayesian Analysis of Microarrays (EBAM) differentially expressed metabolites were identified. The representations of the putative metabolite peaks on the metabolic pathway maps were performed using VANTED (Visualization and Analysis of Networks containing Experimental Data) software [25]. The pathway maps are based on metabolic pathways known to exist in human cells as per information in KEGG database (http://www.genome.jp/kegg/).

Results

Characteristics of infected patients

In order to obtain metabolic markers that can differentiate *Ov*-infected and healthy controls, equal numbers (n=10) of plasma samples from *Ov*-infected and healthy volunteers were analyzed by CE-TOFMS. Clinically the infected individuals had microfilarial counts

between 50-95 mf/mg of skin and were highly positive to the Ov16 specific IgG4 and negative for *W. bancrofti* (Wb123) (tested previously [9, 26]). In contrast the normal healthy individuals had no detectable levels of IgG4 antibodies to Ov16 and Wb123.

Comparative metabolite profiling of serum from infected and healthy individuals

CE-TOFMS measurement of the plasma samples (n=20) from healthy controls and Ovinfected individuals resulted in the detection of 286 peaks of which 170 peaks (119 in cationic mode and 51 in anionic mode) were annotated based on the library of standards and known peaks (Figure 1A, Table 2) with an additional 116 being unknown peaks. Furthermore, putative metabolites could be assigned to peaks based on matches to KEGG, HMDB and HMT peptide databases leaving total of 58 ‘unknown’ metabolites with no matches.

The metabolites were broadly grouped into four categories: (1) Known, (2) potential identifications (based on matches to KEGG, HMDB and peptide databases), (3) Knownunknowns (commonly observed peaks with no annotation, Table 3) and (4) Unknown (no matches to any database). Absolute quantification was performed for 110 metabolites including glycolytic and TCA cycle intermediates, amino acids and nucleic acids (Table 4). As shown in figure 1B, metabolites from all four groups were detected in both the control and infected samples (orange), with a small proportion detected exclusively in the control (blue) or infected individuals (red). Multivariate analyses indicated clear separation between the Onchocerca-infected and control groups in the two-dimensional PCA score plot (Figure 1C), driven by the elevated levels of cluster of metabolites in the control or infected individuals (Figure 1D).

Metabolic changes in infected individuals

Subsets of the metabolites (known and unknown) were detected exclusively in the Ov-infected samples or at significantly higher/lower levels in comparison to uninfected samples. Among the metabolites that were detected (VIP score ≥1) exclusively in either group, the Ov-infected individuals featured the unknown metabolites A_0138, A_0152, A_0159, C_0183; the potential metabolites L-cysteinylglycine disulfide (A_0108), 3b-16a-dihydroxyandrostenone sulfate (A_0136), and hexadecanoic acid (A_0090); and inosine (C_0163) as the sole known metabolite (Figure 2A). In contrast, the unknown metabolites A_0120, A_0124, A_0128, A_0130, A_0132; the potential metabolites ecgonine, histidyl-glycine, adenine, 1-methylguanosine, Nacetylgalactosamine, glutarate, dihydrolipoamide, monoisobutyl phthalic acid, 2-furoate, 2- Ethylhexyl phthalate, 2-amino-3,7-dideoxy-D-threo-hept-6-ulosonic acid, 2,3-dinor-8-isoprostaglandin F2 alpha, and 13-L-hydroperoxylinoleic acid were either not detectable or significantly lower in the infected individuals compared to the uninfected individuals. The unknown metabolites C_0135, C_0172, C_0006, C_0028, C_0080, A_0097 and A_0109 were significantly decreased (VIP score >1) in infected samples with the exception of A_0004 (Figure 2B).

A total of 35 metabolites were observed to be differentially detected (2-fold) by Welch’s T-test (Figure 2C). Serotonin, inosine, isoleucyl-alanine, taurine, hypoxanthine, pipecolic acid, cysteine were also confirmed by empirical Bayesian analysis of microarray (EBAM)

analyses with a posterior value of 0.9 and FDR of 0.017 (Figure 2D) as significantly elevated metabolites in the Ov-infected group. Adenine, glycerol-3-phosphate, cyclohexylamine, choline, glycerophosphocholine were also confirmed by EBAM analyses with a posterior value of 0.9 and FDR of 0.017 (Figure 2D) as significantly elevated metabolites in the uninfected control group

Pathway analysis

The metabolites identified represent perturbations in multiple pathways that include those involved in the metabolism of purines, lipids, tryptophan, taurine, and hypotaurine (Figure 3A). The alteration in branched chain aromatic amino acid and lipid metabolism was due primarily to the decreased levels of choline and glycerophosphocholine in the Ov-infected individuals and to the increased levels of pipecolic acid, tryptophan, kynurenine, serotonin and α-aminoisobutyric acid) (Figure 3B). In addition, the Ov-infected group had significantly decreased levels of tryptophan, tyrosine, arginine, glutamic acid, threonine and valine (Figure S1A) that also relates to the metabolic pathways of arginine, proline, glycine, serine and threonine, Metabolite set enrichment analysis (MSEA) of the known metabolites in addition to the pathways represented in figure 3A, indicated an enrichment of excitatory neural signaling through 5-hydroxytryptamine receptor, serotonin, and phenylacetate metabolism (Figure S1B).

Discussion

Host-pathogen interactions have largely been studied using genomics, transcriptomics and proteomics. More recently, analyses of small metabolites using metabolomics is gaining importance. Infection or disease condition(s) exert considerable impact on the host metabolic profiles. The alterations in the host metabolic profiles may reflect the need for the parasite(s) to create a hospitable niche while competing with the host for nutrients and carbon sources. The metabolic profile of the host serum provides an important window towards understanding the biological changes that occur during infection. Metabolite separation and identification by mass spectrometry (MS) coupled with gas chromatography (GC) and liquid chromatography (LC) have been the most widely used methods, though capillary electrophoresis (CE) has gained increased interest [27]. While each of the techniques has its strengths, weaknesses and challenges [28], the CE approach is well-suited for the separation of polar and ionic molecules. The advantages of CE-MS are: (1) minimal sample and solvent requirement, (2) minimal sample processing and (3) speed. Because of its ability to profile amino acids, amines, small peptides and related metabolites in body fluids, with high selectivity and sensitivity, CE-TOFMS has been described as a powerful tool for clinical analysis [21, 29].

The metabolome is a complex and dynamic process that reflects the metabolism and its variations influenced by numerous intrinsic and extrinsic factors such as food, medications or infection. For practical purposes, the biochemical features in metabolomic data are expected to be within the normal physiological ranges, with just a select few that may be associated with the conditions or phenotypes of interest. The significant differences of specific metabolites between the Ov-infected and the control groups are likely mediated by

infection, as the levels of stable known metabolites did not vary between the groups (Figure S2). Because of the vast nature of the metabolic pathways, the discussion is limited to the observations that relate to known phenomena of host-parasite interactions in filarial infections.

Factors affecting the metabolites

The observations from this exploratory study of *Ov*-infected and -uninfected individuals need to be further explored in a hypothesis-driven approach to test and validate the significant metabolites in the context of diet, other infections, and the microbiomes influencing their altered levels. For example, among the metabolites that were highly elevated in the control sera were citric acid, cic-aconitic acid and isocitric acid, all members of the TCA cycle. Though significant differences in the metabolites from glucose and citrate metabolism have been described, the extremely high levels in the control group in this study are likely to be influenced largely by 1) blood collection protocol differences, 2) or possible increased aconitase activity in the infected individuals, 3) consumption of citrate towards the increased fatty acid synthesis or 4) diet. Cyclohexylamine a metabolite of cyclamate also found in elevated levels in control group is likely to be influenced by diet and microbiome. While the potential sources of cyclamate in diet include tabletop sweeteners, beverages, fruit juices, chewing gum, salad dressings, gelatin desserts, and jellies and jams, cyclamate is not metabolized by mammalian tissues but rather the microflora of the gut [30]. Because the samples tested were frozen archived plasma prior to the mass drug administration programs, the influence of medications affecting the metabolites needs to be evaluated in a targeted metabolomic approach.

Scavenging of intermediates

Because many helminth parasites have definitive and intermediate hosts, they exhibit adaptations to their metabolic pathways that enable increased ATP generation under varying temperatures and anaerobic conditions. Metabolic enzymes of the central carbon metabolism (glycolysis, Krebs TCA cycle, electron transport chain and associated pathways) are crucial and inhibitors of these common pathways affects not only the pathogen(s) but also the host and other organisms, and hence are unlikely to gain potential as drugs. Nevertheless, few structural differences between the host and parasite enzymes indicate considerable possibilities for further advances (reviewed in [31]).

Triose phosphate isomerase is one of the most abundant proteins in the excretorysecretory proteins of filarial parasites [32-34] and catalyzes the interconversion of glyceraldehyde-3-phosphate and dihydroxyacetone phosphate (DHAP) that end up in pyruvate. Though both glyceraldehyde-3-phosphate and DHAP were not detected, the precursor glycerol-3-phosphate was significantly lower in the Ov-infected individuals. The mitochondrial glycerol-3- phosphate dehydrogenase-2 converts glycerol-3-phosphate back to DHAP to contribute to oxidative phosphorylation. Incidentally, stage-specific transcriptional and proteomic data indicate enrichment of oxidative phosphorylation in the microfilarial stages of *Ov* [16]. Interestingly, a hypothetical protein OVOC3987 has its best match to sn-3-glycerol-3-phosphate transporter (GlpT) in the PRK database. It needs to be ascertained whether glycerol-3-phosphate is taken up as an intermediate metabolite towards energy

needs or towards osmotic stress [35]. Glycerol-3- phosphate is also produced by the breakdown of glycerophosphocholine to choline.

Glycerophosphocholine not only functions as an osmolyte [36] and as a metabolic precursor of phospholipids, but also as a rapid source of choline - a biosynthetic precursor of acetylcholine to the brain. Further, the filarial parasites secrete a number of glycoproteins that contain phosphorylcholine (PC) [37, 38] that is a precursor of choline in the glycine, serine and threonine metabolism pathways and is an intermediate between choline and cytidine-diphosphate choline in the glycerophospholipid metabolic pathway. Although studies with ES-62, a PCcontaining filarial glycoprotein demonstrated the choline kinase dependent transfer of PC to the glycoprotein [39], the role of cytidine diphosphate-choline (CDP-choline) and phosphatidylcholine as potential donors of the PC were not conclusive [40]. Moreover, NMR studies of *Brugia malayi* demonstrated glycerophosphoryl-ethanolamine, glycerophosphocholine and phosphoenolpyruvate as the major metabolites and probably the main energy reserves [41]. Current evidence suggest this adaptation of energy reserves is limited to filarial parasites, as their levels are comparatively lower in other helminths [42-47].

Metabolic reconstruction analysis [48] indicated that *Ov* could possibly be dependent on the conversion of guanine and adenine to deoxyguanosine and deoxyadenosine and hence likely to be a target using inhibitors of purine-nucleoside phosphorylase. The lower levels of adenine in the Ov-infected individuals suggests the utilization of the extracellular adenine by *Ov* in addition to the potential contribution of *Wolbachia* to the parasite's purine metabolic needs. If *Loa loa*-infected individuals also have decreased levels of purines, the extracellular nucleotide pool would be the likely source given the absence of *Wolbachia* in *L. loa*. Similarly, the altered levels of arginine, glutamate and threonine (Figure S1A) indicate a possible dependence of *Ov* on salvaging these amino acids from the host.

Interestingly, limited data on Gly-Glu dipeptide suggest its possible role as a neurotrophic factor [49]. Similarly, pipecolic acid - a byproduct of the lysine metabolism that occurs through the saccharopine pathway in the liver or pipecolate pathway in the brain has been associated with pyridoxine-dependent epilepsy and peroxisomal disorders. L-pipecolic acid influences the activity of γ-aminobutyric acid (GABA) [50]; and is also thought to be a factor responsible for hepatic encephalopathy [51, 52]. Whether pipecolic acid originates from food intake or from mammalian or intestinal bacterial metabolism is uncertain. Interestingly, the enzymatic machinery required for the synthesis of pipecolic acid is also present in nematodes [53].

Nematode-derived metabolites

Pathway analysis of the Ov genome [48] identified enzymatic reactions and products of *O. volvulus*, some of which are not present in human host. Further, the small molecule identifier database (SMID DB; http://smid-db.org) houses 179 small molecules from *C.elegans* and other nematodes [54, 55]. These small molecules derived from building blocks of primary metabolic pathways including lipid, amino acid and nucleoside pathways can exert diverse biological functions via conserved signaling cascades, including insulin signaling, TGF-b signaling, steroid biosynthesis, nuclear hormone receptors [56, 57]. It will

be interesting to see if metabolite analyses of *O. volvulus* reveals similar or any additional nematode-derived metabolites that could be the source of some of the unknown metabolites found in the human serum. For example, A_0084 and C_0153 have similar masses with an ascaroside (ascr#2) that is dauer-inducing and male attractant [58].

It should be noted that the present study has several limitations. First, the total sample size of the present study (n=20) was relatively small. Secondly, CE-TOFMS is not very effective for analyzing neutral metabolites and large molecules and hence parallel analyses with LC-MS, GC-MS and NMR approaches can greatly expand the metabolite coverage. Thirdly, the influence of other coincident helminth infection(s), diet and microbiomes on the metabolites were not able to be studied. Although the metabolites' composition is highly dynamic and the contribution by the parasite or the host needs to be carefully controlled, the dataset and information provided is a framework that can help drive validation studies in the future.

Supplementary Material

Refer to Web version on PubMed Central for supplementary material.

Acknowledgments

Funding:

This work was funded in part by the Division of Intramural Research (DIR) of the National Institute of Allergy and Infectious Diseases, National Institutes of Health; and the Bill and Melinda Gates Foundation.

References

1. Centers for Disease, C. and Prevention. Progress toward elimination of onchocerciasis in the Americas - 1993-2012. MMWR Morb Mortal Wkly Rep. 2013; 62(20):405–8. [PubMed: 23698606]
2. WHO. African Programme for Onchocerciasis Control: progress report, 2013-2014. Wkly Epidemiol Rec. 2014; 89(49):551–60. [PubMed: 25485343]
3. Keenan JD, et al. Elimination and eradication of neglected tropical diseases with mass drug administrations: a survey of experts. PLoS Negl Trop Dis. 2013; 7(12):e2562. [PubMed: 24340111]
4. Kim YE, et al. Control, elimination, and eradication of river blindness: scenarios, timelines, and ivermectin treatment needs in Africa. PLoS Negl Trop Dis. 2015; 9(4):e0003664. [PubMed: 25860569]
5. Vlaminck J, Fischer PU, Weil GJ. Diagnostic Tools for Onchocerciasis Elimination Programs. Trends Parasitol. 2015; 31(11):571–82. [PubMed: 26458784]
6. Taylor HR, et al. Reliability of detection of microfilariae in skin snips in the diagnosis of onchocerciasis. Am J Trop Med Hyg. 1989; 41(4):467–71. [PubMed: 2802024]
7. Zimmerman PA, Toe L, Unnasch TR. Design of Onchocerca DNA probes based upon analysis of a repeated sequence family. Mol Biochem Parasitol. 1993; 58(2):259–67. [PubMed: 8479450]
8. Golden A, et al. A Recombinant Positive Control for Serology Diagnostic Tests Supporting Elimination of Onchocerca volvulus. PLoS Negl Trop Dis. 2016; 10(1):e0004292. [PubMed: 26745374]
9. Steel C, et al. Rapid Point-of-Contact Tool for Mapping and Integrated Surveillance of Wuchereria bancrofti and Onchocerca volvulus Infection. Clin Vaccine Immunol. 2015; 22(8):896–901. [PubMed: 26018537]
10. Steel C, et al. Rapid Wuchereria bancrofti-specific antigen Wb123-based IgG4 immunoassays as tools for surveillance following mass drug administration programs on lymphatic filariasis. Clin Vaccine Immunol. 2013; 8(20):1155–61.

11. Weil GJ, et al. A rapid-format antibody card test for diagnosis of onchocerciasis. J Infect Dis. 2000; 6(182):1796–9.
12. Lobos E, et al. An immunogenic Onchocerca volvulus antigen: a specific and early marker of infection. Science. 1991; 251(5001):1603–5. [PubMed: 2011741]
13. Bottomley C, et al. Modelling Neglected Tropical Diseases diagnostics: the sensitivity of skin snips for Onchocerca volvulus in near elimination and surveillance settings. Parasit Vectors. 2016; 9(1): 343. [PubMed: 27301567]
14. Quintana JF, et al. Extracellular Onchocerca-derived small RNAs in host nodules and blood. Parasit Vectors. 2015; 8:58. [PubMed: 25623184]
15. Tritten L, et al. Detection of circulating parasite-derived microRNAs in filarial infections. PLoS Negl Trop Dis. 2014; 7(8):e2971.
16. Bennuru S, et al. Stage-Specific Transcriptome and Proteome Analyses of the Filarial Parasite Onchocerca volvulus and Its Wolbachia Endosymbiont. MBio. 2016; 7(6)
17. Denery JR, et al. Metabolomics-based discovery of diagnostic biomarkers for onchocerciasis. PLoS Negl Trop Dis. 2010; 4(10)
18. Globisch D, et al. Onchocerca volvulus-neurotransmitter tyramine is a biomarker for river blindness. Proc Natl Acad Sci U S A. 2013; 110(11):4218–23. [PubMed: 23440222]
19. Globisch D, et al. Litomosoides sigmodontis: a jird urine metabolome study. Bioorg Med Chem Lett. 2015; 25(24):5804–7. [PubMed: 26573416]
20. Lagatie O, et al. Evaluation of the diagnostic potential of urinary NAcetyltyramine-O,beta-glucuronide (NATOG) as diagnostic biomarker for Onchocerca volvulus infection. Parasit Vectors. 2016; 9(1):302. [PubMed: 27216752]
21. Soga T, et al. Quantitative metabolome analysis using capillary electrophoresis mass spectrometry. J Proteome Res. 2003; 2(5):488–94. [PubMed: 14582645]
22. Ogata H, et al. KEGG: Kyoto Encyclopedia of Genes and Genomes. Nucleic Acids Res. 1999; 27(1):29–34. [PubMed: 9847135]
23. Wishart DS, et al. HMDB: a knowledgebase for the human metabolome. Nucleic Acids Res. 2009; 37(Database issue):D603–10. [PubMed: 18953024]
24. Xia J, Wishart DS. Using MetaboAnalyst 3.0 for Comprehensive Metabolomics Data Analysis. Curr Protoc Bioinformatics. 2016; 55:14 10 1–14 10 91.
25. Rohn H, et al. VANTED v2: a framework for systems biology applications. BMC Syst Biol. 2012; 6:139. [PubMed: 23140568]
26. Golden A, et al. Extended result reading window in lateral flow tests detecting exposure to Onchocerca volvulus: a new technology to improve epidemiological surveillance tools. PLoS One. 2013; 8(7):e69231. [PubMed: 23935960]
27. Ramautar R, Somsen GW, de Jong GJ, et al. CE-MS for metabolomics: developments and applications in the period 2010-2012. Electrophoresis. 2013; 34(1):86–98. [PubMed: 23161106]
28. Biology, MiM, et al. Mass Spectrometry in Metabolomics. In: Walker, JM., editor. Methods in Molecular Biology. Humana Press; 2014.
29. Staub A, et al. CE-TOF/MS: fundamental concepts, instrumental considerations and applications. Electrophoresis. 2009; 30(10):1610–23. [PubMed: 19441039]
30. Bopp BA, Sonders RC, Kesterson JW, et al. Toxicological aspects of cyclamate and cyclohexylamine. Crit Rev Toxicol. 1986; 16(3):213–306. [PubMed: 2420530]
31. Timson DJ, et al. Metabolic Enzymes of Helminth Parasites: Potential as Drug Targets. Curr Protein Pept Sci. 2016; 17(3):280–95. [PubMed: 26983888]
32. Hewitson JP, et al. The secreted triose phosphate isomerase of Brugia malayi is required to sustain microfilaria production in vivo. PLoS Pathog. 2014; 10(2):e1003930. [PubMed: 24586152]
33. Hewitson JP, et al. The secretome of the filarial parasite, Brugia malayi: proteomic profile of adult excretory-secretory products. Mol Biochem Parasitol. 2008; 160(1):8–21. [PubMed: 18439691]
34. Bennuru S, et al. Brugia malayi excreted/secreted proteins at the host/parasite interface: stage- and gender-specific proteomic profiling. PLoS Negl Trop Dis. 2009; 3(4):e410. [PubMed: 19352421]
35. Possik E, Pause A, et al. Glycogen: A must have storage to survive stressful emergencies. Worm. 2016; 5(2):e1156831. [PubMed: 27383221]

36. Gallazzini M, Burg MB, et al. What's new about osmotic regulation of glycerophosphocholine. Physiology (Bethesda). 2009; 24:245–9. [PubMed: 19675355]
37. Maizels RM, Burke J, Denham DA, et al. Phosphorylcholine-bearing antigens in filarial nematode parasites: analysis of somatic extracts, in-vitro secretions and infection sera from Brugia malayi and B. pahangi. Parasite Immunol. 1987; 9(1):49–66. [PubMed: 2436131]
38. Haslam SM, et al. Structural studies of N-glycans of filarial parasites. Conservation of phosphorylcholine-substituted glycans among species and discovery of novel chito-oligomers. J Biol Chem. 1999; 274(30):20953–60. [PubMed: 10409642]
39. Houston KM, Harnett W, et al. Mechanisms underlying the transfer of phosphorylcholine to filarial nematode glycoproteins--a possible role for choline kinase. Parasitology. 1999; 118(pt 3):311–8. [PubMed: 10205808]
40. Houston KM, Harnett W, et al. Structure and synthesis of nematode phosphorylcholine-containing glycoconjugates. Parasitology. 2004; 129(Pt 6):655–61. [PubMed: 15648688]
41. Shukla-Dave A, et al. Metabolite mapping of human filarial parasite, Brugia malayi with nuclear magnetic resonance. Magn Reson Imaging. 1999; 17(10):1503–9. [PubMed: 10609999]
42. Matthews PM, et al. 31P-NMR studies of metabolite compartmentation in Fasciola hepatica. Biochim Biophys Acta. 1985; 845(2):178–88. [PubMed: 3995088]
43. Mansour TE, et al. A 31P-nmr study of the intact liver fluke Fasciola hepatica. Biochim Biophys Acta. 1982; 721(4):336–40. [PubMed: 7159598]
44. Platzer EG, et al. High energy phosphate metabolites observed by NMR in infective larvae of Haemonchus contortus. J Parasitol. 1995; 81(3):434–8. [PubMed: 7776130]
45. Thompson SN, Platzer EG, Lee RW, et al. Bioenergetics in a parasitic nematode, Steinernema carpocapsae, monitored in vivo by flow NMR spectroscopy. Parasitol Res. 1991; 77(1):86–90. [PubMed: 1994374]
46. Thompson SN, Platzer EG, Lee RW, et al. Phosphoglycerides and derivatives in Taenia crassiceps examined by 31P NMR spectroscopy. J Parasitol. 1988; 74(1):194–6. [PubMed: 3357104]
47. Thompson SN, Platzer EG, Lee RW, et al. In vivo 31P NMR spectrum of Hymenolepis diminuta and its change on short-term exposure to mebendazole. Mol Biochem Parasitol. 1987; 22(1):45–54. [PubMed: 3807950]
48. Cotton JA, et al. The genome of Onchocerca volvulus, agent of river blindness. Nat Microbiol. 2016; 2:16216. [PubMed: 27869790]
49. Koelle GB, Sanville UJ, Wall SJ, et al. Glycyl-L-glutamine, a precursor, and glycyl-L-glutamic acid, a neurotrophic factor for maintenance of acetylcholinesterase and butyrylcholinesterase in the preganglionically denervated superior cervical ganglion of the cat in vivo. Proc Natl Acad Sci U S A. 1985; 82(15):5213–7. [PubMed: 3860856]
50. Feigenbaum P, Chang YF, et al. Pipecolic acid antagonizes barbiturateenhanced GABA binding to bovine brain membranes. Brain Res. 1986; 372(1):176–9. [PubMed: 3011206]
51. Fujita T, Hada T, Higashino K, et al. Origin of D- and L-pipecolic acid in human physiological fluids: a study of the catabolic mechanism to pipecolic acid using the lysine loading test. Clin Chim Acta. 1999; 287(1-2):145–56. [PubMed: 10509903]
52. Fujita T, et al. Plasma levels of pipecolic acid, both L- and D-enantiomers, in patients with chronic liver diseases, especially hepatic encephalopathy. Clin Chim Acta. 1999; 287(1-2):99–109. [PubMed: 10509899]
53. Umair S, Bland RJ, Simpson HV, et al. Lysine catabolism in Haemonchus contortus and Teladorsagia circumcincta. Exp Parasitol. 2012; 131(1):101–6. [PubMed: 22459625]
54. Yim JJ, et al. Nematode signaling molecules derived from multimodular assembly of primary metabolic building blocks. Org Lett. 2015; 17(7):1648–51. [PubMed: 25782998]
55. Bose N, et al. Complex small-molecule architectures regulate phenotypic plasticity in a nematode. Angew Chem Int Ed Engl. 2012; 51(50):12438–43. [PubMed: 23161728]
56. von Reuss SH, Schroeder FC, et al. Combinatorial chemistry in nematodes: modular assembly of primary metabolism-derived building blocks. Nat Prod Rep. 2015; 32(7):994–1006. [PubMed: 26059053]
57. Ludewig AH, Schroeder FC, et al. Ascaroside signaling in C. elegans. WormBook. 2013:1–22.

58. DB. CeSMIDS. 2011

Highlights

- Metabolic changes associated with human *O. volvulus* infection identified
- Specific metabolites may be potential biomarkers of active infection
- Metabolic pathways influenced by infection inferred

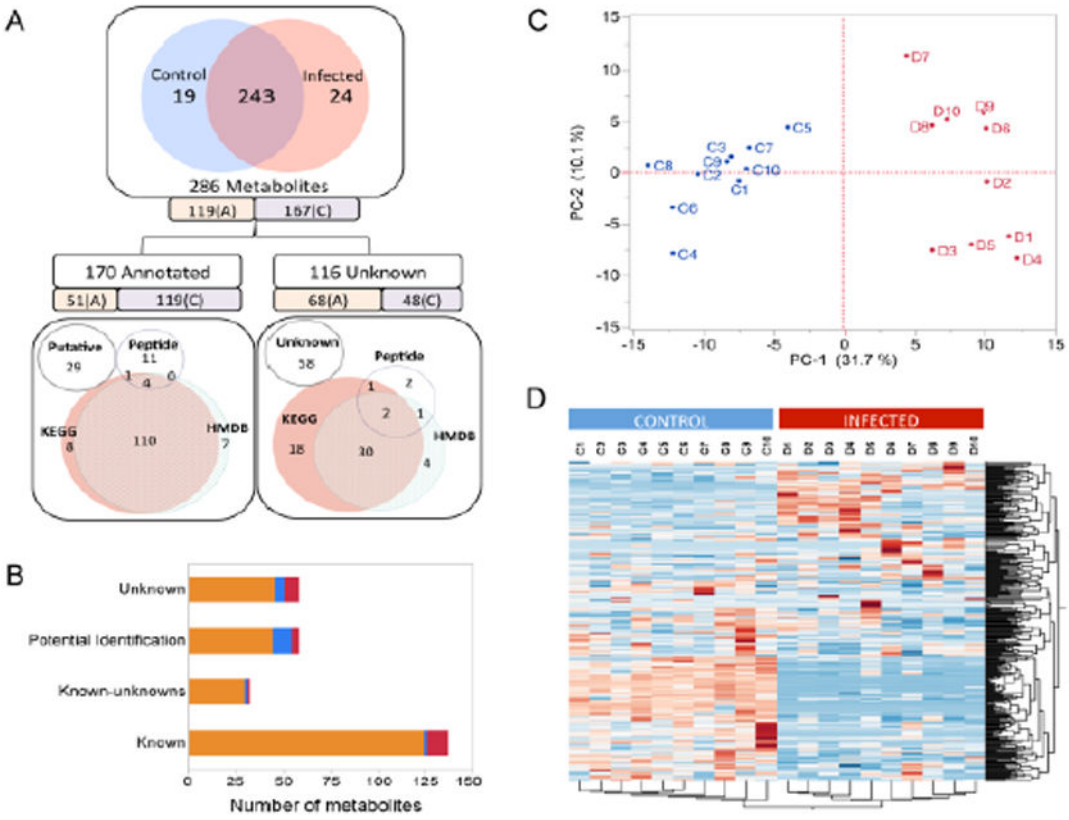

Figure 1.

Ov infected serum metabolites. A) The distribution of 286 metabolites identified in control and infected samples in the cation (C) or anion (A) modes. 170 metabolites were annotated based on KEGG, HMDB, HMT peptide library, and putative metabolites. 116 unknown metabolites with no identifications or likely inferences from KEGG, HMDB databases. B) Bar graph depicts the number of unknown, potential identifications, known-unknowns and known metabolites in the infected alone (red), control (blue) or both (orange). C) Principal component score plot showing the separation of infected (D1-10) and control (C1-10) groups. D) Heatmap shows the unsupervised hierarchical clustering of the metabolites.

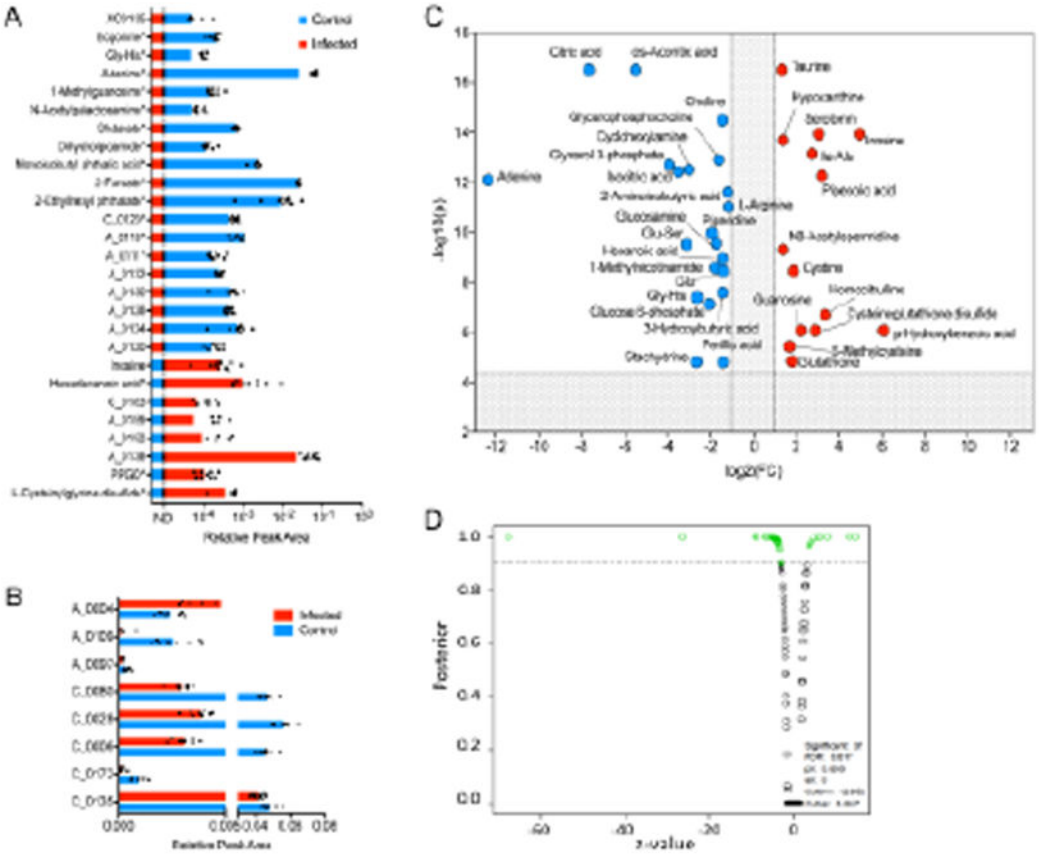

Figure 2.

Significant metabolites. A) The bar graph shows the relative peak area of the metabolites identified exclusively in the control (blue) or infected (red) samples. The dotted line with 'ND' denotes not detected. Asterisk denotes potential identifications of the metabolites. B) The bar graph shows the relative peak area of the unknown metabolites that were significantly altered in the infected samples. C) Volcano plot showing the significant metabolites with log 2-fold change on the x-axis and -log 10 of the p-values on the y-axis. The shaded area corresponds to non-significant metabolites. D) EBAM plot of the significant metabolites. The points above the dotted line correspond to the metabolites with a posterior probability of 0.9 of being differentially identified. The fudge factor (a0=0) and Delta = 0.9, with an FDR of 0.01 identified 37 significantly altered metabolites.

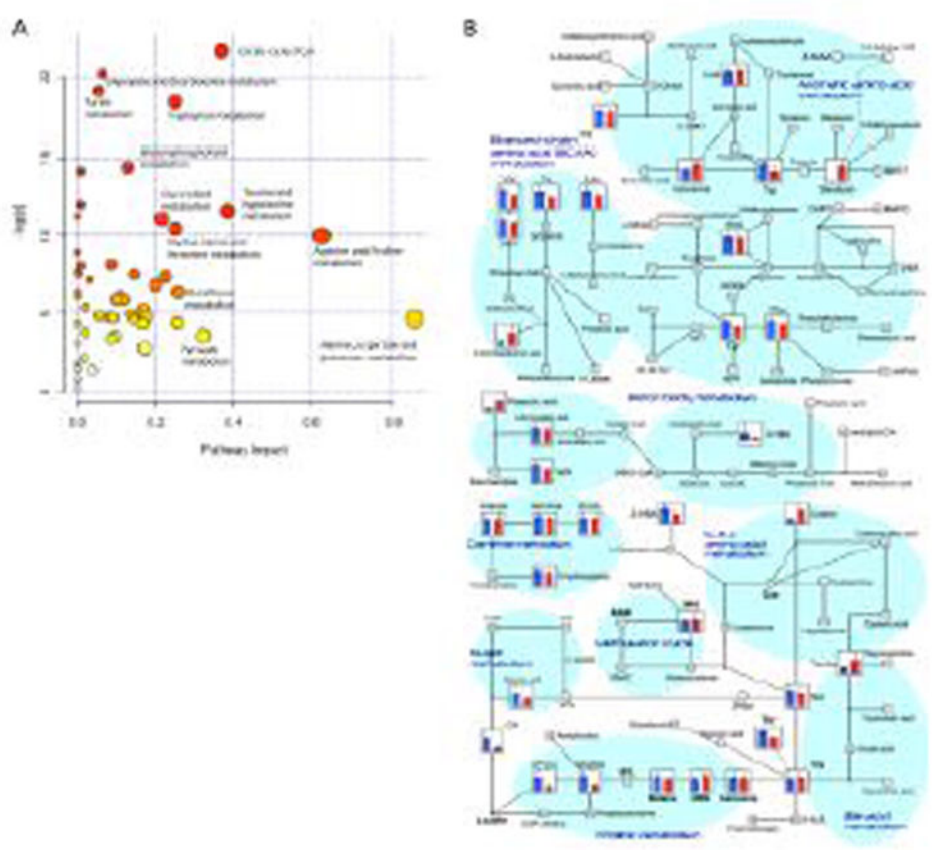

Figure 3.

Metabolome view. A) The scattered bubble plot shows all the matched pathways (mapped metabolites) arranged by the p-values from pathway enrichment analysis on the y-axis and the pathway impact values from the pathway topology analysis on the x-axis. The node color is based on its p-value and the node radius is determined based on the pathway impact values. B) Graphical representation of the significant metabolites mapped to known pathways of lipid and amino acid metabolism highlighting the choline, phosphorylcholine and pipecolic acid; and branched chain aromatic amino acids GABA, serotonin, tryptophan and kynurenine. The bar graphs at each node represent the metabolite levels in the control (blue) and infected (red) samples

Table 1

Sample serology

Groups	MF/mg of skin	Ov16 IgG4	Wb123 IgG4
Infected-1	78	+	-
Infected-2	84	+	-
Infected-3	95	+	-
Infected-4	70	+	-
Infected-5	84	+	-
Infected-6	65	+	-
Infected-7	75	+	-
Infected-8	50	+	-
Infected-9	95	+	-
Infected-10	95	+	-
Control-1	-	-	-
Control-2	-	-	-
Control-3	-	-	-
Control-4	-	-	-
Control-5	-	-	-
Control-6	-	-	-
Control-7	-	-	-
Control-8	-	-	-
Control-9	-	-	-
Control-10	-	-	-

Table 2

Putative Metabolites

ID	Compound name	Relative Area				Comparative Analysis		
		Control		Disease		Disease vs Control		
		Mean	S.D.	Mean	S.D.	Ratio¶	p-value#	
A_0029	*p*-Hydroxybenzoic acid	N.D.	N.A.	1.4E-03	9.5E-04	1<	N.A.	
A_0053	Azelaic acid	N.D.	N.A.	3.5E-03	N.A.	1<	N.A.	
A_0075	Ribulose 5-phosphate	N.D.	N.A.	1.6E-04	N.A.	1<	N.A.	
C_0034	Homoserine	N.D.	N.A.	6.0E-05	N.A.	1<	N.A.	
C_0051	Gly-Gly	N.D.	N.A.	1.5E-03	N.A.	1<	N.A.	
C_0092	Betonicine	N.D.	N.A.	2.6E-03	N.A.	1<	N.A.	
C_0108	Serotonin	N.D.	N.A.	9.1E-05	4.2E-05	1<	N.A.	
C_0158	XC0088	N.D.	N.A.	3.3E-04	3.2E-04	1<	N.A.	
C_0163	Inosine	N.D.	N.A.	3.4E-04	2.4E-04	1<	N.A.	
C_0168	Guanosine	N.D.	N.A.	8.9E-05	6.7E-05	1<	N.A.	
C_0175	Glutathione (GSSG)_divalent	N.D.	N.A.	7.8E-05	4.0E-05	1<	N.A.	
C_0185	Cysteine glutathione disulfide	N.D.	N.A.	1.5E-04	9.0E-05	1<	N.A.	
C_0173	XC0120	1.1E-04	4.0E-05	1.1E-03	5.6E-04	9.6	4.2E-04	***
C_0041	Pipecolic acid	8.9E-04	7.8E-04	8.2E-03	7.8E-03	9.2	0.015	*
C_0128	Glu-Gly	7.0E-05	1.3E-05	5.4E-04	7.2E-04	7.6	0.530	
	Glu-Gly							
C_0116	Homocitrulline	1.1E-04	4.4E-05	5.5E-04	1.2E-03	5.2	0.301	
A_0026	6-Hydroxyhexanoic acid	9.7E-05	4.3E-05	4.2E-04	4.4E-04	4.3	0.329	
C_0148	Cystine	1.2E-03	5.0E-04	4.5E-03	2.2E-03	3.7	8.8E-04	***
C_0055	*S*-Methylcysteine	6.3E-04	3.6E-04	2.0E-03	1.9E-03	3.2	0.047	*
C_0109	Glucosamine	3.3E-04	5.5E-04	8.9E-04	N.A.	2.7	N.A.	
C_0003	XC0001	1.0E-04	5.5E-05	2.8E-04	2.0E-04	2.7	0.039	*
C_0057	Hypoxanthine	6.2E-04	1.9E-04	1.6E-03	5.1E-04	2.6	9.3E-05	***
C_0018	3-Aminoisobutyric acid	3.5E-04	1.5E-04	9.1E-04	7.3E-04	2.6	0.041	*

ID	Compound name	Relative Area				Comparative Analysis		
		Control		Disease		Disease vs Control		
		Mean	S.D.	Mean	S.D.	Ratio¶	p-value#	
C_0038	Taurine	1.8E-03	3.0E-04	4.4E-03	2.3E-03	2.5	0.005	**
A_0063	*S*-Sulfocysteine	1.2E-04	9.9E-06	2.9E-04	1.0E-04	2.5	0.040	*
A_0005	Lactic acid	9.0E-02	2.9E-02	2.1E-01	1.3E-01	2.3	0.019	*
C_0122	Ile-Ala	6.2E-05	5.4E-06	1.4E-04	5.8E-05	2.2	0.002	**
C_0114	N^8-Acetylspermidine	2.9E-05	6.0E-06	6.2E-05	1.9E-05	2.1	6.9E-04	***
C_0164	XC0107	3.7E-04	1.7E-04	7.7E-04	4.2E-04	2.1	0.018	*
A_0095	N^2-Phenylacetylglutamine	2.3E-04	1.1E-04	4.2E-04	2.9E-04	1.9	0.072	
C_0005	Trimethylamine *N*-oxide	2.8E-03	2.5E-03	4.8E-03	3.8E-03	1.7	0.178	
C_0137	XC0061	2.8E-04	1.1E-04	4.4E-04	2.7E-04	1.6	0.119	
C_0117	XC0045	1.5E-04	4.2E-05	2.2E-04	1.9E-04	1.5	0.312	
C_0015	GABA	7.4E-05	1.2E-05	1.1E-04	8.5E-05	1.5	0.399	
C_0132	Kynurenine	4.3E-04	6.9E-05	6.3E-04	1.4E-04	1.5	0.002	**
C_0050	Asn	6.1E-03	1.6E-03	8.9E-03	4.0E-03	1.5	0.065	
A_0003	Pyruvic acid	3.0E-03	1.2E-03	4.3E-03	1.4E-03	1.4	0.069	
C_0124	SDMA	1.5E-04	5.8E-05	2.2E-04	6.3E-05	1.4	0.033	*
A_0092	Glucose 6-phosphate	1.8E-04	9.6E-05	2.5E-04	N.A.	1.4	N.A.	
C_0104	N^5-Ethylglutamine	3.1E-04	1.8E-04	4.3E-04	3.4E-04	1.4	0.346	
A_0017	2-Hydroxyvaleric acid	1.3E-03	6.3E-04	1.7E-03	1.3E-03	1.3	0.387	
C_0016	*N,N*-Dimethylglycine	9.3E-04	2.5E-04	1.2E-03	2.9E-04	1.3	0.041	*
A_0027	Malic acid	1.2E-03	5.2E-04	1.5E-03	6.0E-04	1.3	0.222	
C_0123	ADMA	1.6E-04	2.3E-05	2.0E-04	5.1E-05	1.3	0.035	*
C_0118	XC0046	1.1E-04	3.9E-05	1.4E-04	5.5E-05	1.2	0.212	
A_0028	Threonic acid	1.4E-03	3.7E-04	1.7E-03	4.3E-04	1.2	0.079	
C_0013	Glycerol	1.1E-01	2.7E-02	1.4E-01	5.2E-02	1.2	0.173	
A_0023	*N*-Acetylalanine	1.6E-04	3.7E-05	2.0E-04	4.4E-05	1.2	0.054	
A_0014	*N*-Acetylglycine	1.6E-04	7.2E-05	1.9E-04	7.3E-05	1.2	0.309	
A_0019	Benzoic acid	4.9E-04	1.2E-04	6.0E-04	1.3E-04	1.2	0.204	

ID	Compound name	Relative Area				Comparative Analysis	
		Control		Disease		Disease vs Control	
		Mean	S.D.	Mean	S.D.	Ratio[¶]	p-value[#]
A_0072	Myristoleic acid	2.0E-04	1.0E-04	2.4E-04	1.7E-04	1.2	0.590
C_0075	Gln	8.4E-02	2.3E-02	1.0E-01	2.8E-02	1.2	0.177
C_0084	XC0033	3.4E-04	2.8E-04	4.0E-04	4.0E-04	1.2	0.705
A_0006	Isovaleric acid	6.1E-04	3.8E-04	7.0E-04	9.5E-04	1.2	0.880
C_0004	Gly	3.9E-02	1.8E-02	4.5E-02	1.5E-02	1.2	0.420
C_0152	Uridine	9.0E-04	1.3E-04	1.0E-03	2.3E-04	1.1	0.123
C_0037	Nicotinamide	8.6E-05	2.6E-05	9.8E-05	3.5E-05	1.1	0.447
C_0089	Imidazolelactic acid	9.4E-05	4.0E-05	1.1E-04	6.6E-05	1.1	0.704
C_0081	Met	4.6E-03	1.4E-03	5.0E-03	3.9E-03	1.1	0.758
A_0046	Indole-3-acetic acid	1.5E-04	3.5E-05	1.6E-04	7.5E-05	1.1	0.709
A_0025	2-Hydroxy-4-methylvaleric acid	1.5E-04	4.5E-05	1.6E-04	8.4E-05	1.1	0.869
C_0023	XC0008	2.5E-02	6.3E-03	2.6E-02	1.9E-02	1.0	0.862
C_0046	Creatine	1.0E-02	5.0E-03	1.1E-02	8.9E-03	1.0	0.928
C_0119	XC0048	6.8E-05	3.1E-05	6.8E-05	2.0E-05	1.0	0.988
C_0126	*O*-Acetylcarnitine	7.1E-03	2.7E-03	7.1E-03	2.7E-03	1.0	0.983
C_0045	Hydroxyproline	3.0E-03	1.9E-03	3.0E-03	1.3E-03	1.0	0.986
C_0002	Ethanolamine	1.6E-03	1.7E-04	1.6E-03	4.0E-04	1.0	0.949
A_0039	Uric acid	1.8E-02	4.3E-03	1.8E-02	4.3E-03	1.0	0.904
C_0052	Ornithine	1.7E-02	5.4E-03	1.7E-02	1.0E-02	1.0	0.924
A_0088	Ascorbate 2-sulfate	3.5E-04	7.7E-05	3.4E-04	1.3E-04	1.0	0.865
C_0072	γ-Butyrobetaine	1.1E-03	4.2E-04	1.1E-03	5.1E-04	1.0	0.884
C_0167	1-Methyladenosine	7.2E-05	1.5E-05	6.9E-05	1.5E-05	1.0	0.669
A_0049	Homovanillic acid	1.7E-04	5.0E-05	1.6E-04	4.9E-05	1.0	0.719
C_0082	Triethanolamine	7.7E-05	1.5E-05	7.3E-05	2.5E-05	0.9	0.688
C_0142	XC0070	3.0E-04	1.1E-04	2.8E-04	1.1E-04	0.9	0.722
A_0036	Perillic acid	3.9E-04	1.7E-04	3.7E-04	1.2E-04	0.9	0.807
C_0010	Sarcosine	4.0E-04	1.5E-04	3.8E-04	1.2E-04	0.9	0.680

ID	Compound name	Relative Area				Comparative Analysis		
		Control		Disease		Disease vs Control		
		Mean	S.D.	Mean	S.D.	Ratio[¶]	p-value[#]	
C_0096	Carnitine	2.4E-02	4.5E-03	2.2E-02	4.5E-03	0.9	0.428	
A_0062	Lauric acid	4.2E-03	5.0E-04	3.9E-03	6.4E-04	0.9	0.269	
A_0031	Octanoic acid	3.2E-04	5.5E-05	3.0E-04	1.2E-04	0.9	0.540	
A_0082	XA0034	2.6E-04	5.0E-05	2.4E-04	8.2E-05	0.9	0.490	
C_0095	2-Aminoadipic acid	1.6E-04	5.7E-05	1.5E-04	5.8E-05	0.9	0.594	
C_0071	4-Guanidinobutyric acid	7.7E-05	6.0E-05	7.1E-05	7.9E-06	0.9	0.777	
C_0020	Ser	2.4E-02	9.1E-03	2.2E-02	9.6E-03	0.9	0.549	
A_0030	*o*-Hydroxybenzoic acid	4.5E-03	N.A.	4.0E-03	N.A.	0.9	N.A.	
C_0143	Isobutyrylcarnitine	1.3E-04	8.4E-05	1.2E-04	4.4E-05	0.9	0.603	
A_0047	Hippuric acid	6.0E-04	4.4E-04	5.3E-04	3.3E-04	0.9	0.679	
C_0011	Ala	1.1E-01	2.5E-02	9.2E-02	2.7E-02	0.9	0.280	
A_0044	Decanoic acid	3.7E-04	9.1E-05	3.2E-04	1.1E-04	0.9	0.277	
A_0012	2-Oxoisovaleric acid	1.1E-03	3.0E-04	9.6E-04	2.7E-04	0.9	0.254	
A_0068	XA0025	4.3E-04	5.4E-05	3.6E-04	3.3E-05	0.8	0.003	**
C_0097	5-Hydroxylysine	9.0E-05	3.5E-05	7.6E-05	4.1E-05	0.8	0.467	
A_0034	Pelargonic acid	4.3E-04	8.0E-05	3.6E-04	1.1E-04	0.8	0.124	
A_0020	Isethionic acid	1.7E-04	3.9E-05	1.4E-04	5.3E-05	0.8	0.286	
A_0066	3-Indoxylsulfuric acid	7.6E-04	5.1E-04	6.2E-04	2.7E-04	0.8	0.451	
C_0012	β-Ala	6.3E-04	4.6E-04	5.1E-04	1.4E-04	0.8	0.448	
C_0029	Guanidoacetic acid	7.2E-04	2.0E-04	5.7E-04	2.7E-04	0.8	0.177	
A_0015	Succinic acid	9.3E-04	2.2E-04	7.3E-04	2.2E-04	0.8	0.060	
C_0099	Phe	3.5E-02	7.3E-03	2.7E-02	1.2E-02	0.8	0.104	
C_0031	Betaine	2.1E-02	5.9E-03	1.6E-02	4.5E-03	0.8	0.058	
A_0058	Glucuronic acid	1.8E-04	4.4E-05	1.4E-04	3.6E-05	0.8	0.036	*
C_0088	His	2.6E-02	4.5E-03	2.0E-02	5.6E-03	0.8	0.016	*
C_0107	Citrulline	7.8E-03	2.8E-03	5.9E-03	1.9E-03	0.8	0.100	
A_0022	4-Methyl-2-oxovaleric acid	6.2E-03	2.2E-03	4.7E-03	2.4E-03	0.8	0.175	

ID	Compound name	Relative Area				Comparative Analysis		
		Control		Disease		Disease vs Control		
		Mean	S.D.	Mean	S.D.	Ratio[¶]	p-value[#]	
	3-Methyl-2-oxovaleric acid							
C_0144	Butyrylcarnitine	1.0E-04	5.9E-05	7.8E-05	2.9E-05	0.7	0.229	
C_0025	Creatinine	2.3E-02	7.9E-03	1.7E-02	6.7E-03	0.7	0.087	
C_0040	XC0016	3.7E-03	2.3E-03	2.7E-03	1.9E-03	0.7	0.312	
C_0026	Pro	9.3E-02	2.1E-02	6.9E-02	1.7E-02	0.7	0.010	**
C_0047	Leu	9.8E-02	2.9E-02	7.1E-02	3.2E-02	0.7	0.067	
C_0077	Lys	5.3E-02	1.2E-02	3.8E-02	1.1E-02	0.7	0.011	*
A_0021	5-Oxoproline	3.4E-03	1.2E-03	2.4E-03	1.0E-03	0.7	0.064	
C_0159	Dyphylline	9.1E-03	8.2E-04	6.4E-03	1.9E-03	0.7	0.001	**
A_0013	Hexanoic acid	2.8E-04	6.0E-05	1.9E-04	7.2E-05	0.7	0.058	
C_0086	XC0034	2.0E-04	1.6E-04	1.3E-04	7.2E-05	0.7	0.291	
A_0059	Gluconic acid	6.0E-04	1.6E-04	4.1E-04	1.0E-04	0.7	0.005	**
C_0027	XC0011	6.7E-05	1.4E-05	4.5E-05	1.0E-05	0.7	9.5E-04	***
C_0030	Val	1.2E-01	2.6E-02	7.9E-02	2.2E-02	0.7	0.002	**
C_0177	XC0125	2.5E-04	2.2E-04	1.6E-04	N.A.	0.6	N.A.	
C_0166	XC0112	3.5E-04	2.2E-04	2.2E-04	N.A.	0.6	N.A.	
C_0053	Asp	3.1E-03	1.0E-03	2.0E-03	2.5E-03	0.6	0.216	
C_0062	XC0025	2.4E-04	2.0E-04	1.5E-04	5.3E-05	0.6	0.208	
A_0007	2-Hydroxybutyric acid	2.2E-03	7.0E-04	1.4E-03	5.6E-04	0.6	0.007	**
C_0127	XC0055	3.3E-04	3.8E-04	2.0E-04	8.0E-05	0.6	0.311	
C_0021	Diethanolamine	9.4E-04	7.3E-04	5.7E-04	4.3E-04	0.6	0.183	
C_0033	Thr	3.7E-02	1.0E-02	2.2E-02	7.3E-03	0.6	0.002	**
C_0048	Ile	4.9E-02	1.7E-02	2.9E-02	1.4E-02	0.6	0.010	*
C_0001	Urea	4.6E-01	1.3E-01	2.8E-01	6.4E-02	0.6	0.001	**
C_0044	XC0019	8.1E-05	6.8E-05	4.8E-05	1.3E-05	0.6	0.192	
C_0110	Tyr	2.1E-02	4.3E-03	1.2E-02	4.9E-03	0.6	5.2E-04	***
A_0009	Glyceric acid	1.7E-03	1.0E-03	1.0E-03	2.7E-04	0.6	0.053	

ID	Compound name	Relative Area				Comparative Analysis		
		Control		Disease		Disease vs Control		
		Mean	S.D.	Mean	S.D.	Ratio[¶]	p-value[#]	
C_0182	Trp-His	1.0E-04	8.1E-05	5.8E-05	3.0E-05	0.6	0.360	
C_0155	XC0080	1.6E-04	1.3E-04	8.7E-05	7.1E-05	0.6	0.184	
C_0065	1-Methyl-4-imidazoleacetic acid	2.3E-04	1.2E-04	1.3E-04	3.5E-05	0.6	0.073	
C_0161	XC0096	1.9E-04	1.4E-04	1.1E-04	4.3E-05	0.5	0.085	
C_0129	Trp	1.5E-02	2.7E-03	8.2E-03	3.4E-03	0.5	5.6E-05	***
C_0171	XC0119	8.2E-05	5.9E-05	4.3E-05	N.A.	0.5	N.A.	
C_0060	Trigonelline	1.4E-03	1.2E-03	7.4E-04	4.4E-04	0.5	0.108	
C_0170	XC0117	3.1E-04	1.7E-04	1.5E-04	N.A.	0.5	N.A.	
C_0140	XC0067	3.3E-04	7.4E-05	1.6E-04	N.A.	0.5	N.A.	
C_0105	Arg	3.7E-02	1.0E-02	1.7E-02	8.4E-03	0.5	1.4E-04	***
A_0032	2-Oxoglutaric acid	2.3E-03	1.3E-03	1.0E-03	5.5E-04	0.5	0.022	*
C_0017	2-Aminoisobutyric acid	5.8E-03	1.9E-03	2.6E-03	1.3E-03	0.4	4.3E-04	***
	2-Aminobutyric acid							
C_0106	Guanidinosuccinic acid	9.7E-05	5.1E-05	4.2E-05	7.8E-06	0.4	0.071	
C_0058	1-Methylnicotinamide	1.4E-04	5.6E-05	5.3E-05	2.1E-05	0.4	0.002	**
C_0078	Glu	5.4E-02	1.7E-02	2.0E-02	2.0E-02	0.4	7.6E-04	***
C_0169	His-Glu	9.8E-05	2.3E-05	3.7E-05	8.7E-06	0.4	7.3E-04	***
A_0008	3-Hydroxybutyric acid	3.0E-03	3.6E-03	1.1E-03	6.7E-04	0.4	0.136	
C_0019	Choline	3.2E-02	9.6E-03	1.2E-02	3.8E-03	0.4	5.0E-05	***
C_0066	XC0029	2.5E-04	2.2E-04	8.8E-05	1.8E-05	0.4	0.080	
C_0101	3-Methylhistidine	4.3E-03	5.2E-03	1.4E-03	7.0E-04	0.3	0.119	
C_0160	Glycerophosphocholine	1.4E-03	5.0E-04	4.4E-04	2.3E-04	0.3	1.6E-04	***
C_0007	Piperidine	1.0E-03	3.7E-04	3.4E-04	2.9E-04	0.3	3.0E-04	***
A_0104	XA0039	6.6E-04	1.8E-04	2.0E-04	1.6E-04	0.3	1.8E-05	***
C_0146	XC0075	1.5E-04	7.7E-05	4.4E-05	N.A.	0.3	N.A.	
C_0094	N^6-Methyllysine	2.4E-03	3.1E-03	6.4E-04	2.4E-04	0.3	0.116	
C_0085	Guanine	1.1E-04	1.1E-04	3.1E-05	1.2E-05	0.3	0.476	

ID	Compound name	Relative Area				Comparative Analysis		
		Control		Disease		Disease vs Control		
		Mean	S.D.	Mean	S.D.	Ratio[¶]	p-value[#]	
C_0145	Glu-Ser	2.9E-04	1.6E-04	7.5E-05	4.4E-05	0.3	0.005	**
A_0043	Glycerol 3-phosphate	5.2E-04	2.8E-04	1.2E-04	8.4E-05	0.2	0.009	**
C_0014	Cyclohexylamine	5.8E-04	1.7E-04	1.1E-04	8.9E-05	0.2	4.3E-06	***
A_0122	XA0052	9.0E-04	1.9E-04	1.6E-04	N.A.	0.2	N.A.	
C_0067	Stachydrine	1.4E-02	2.0E-02	2.3E-03	1.7E-03	0.2	0.086	
A_0056	Isocitric acid	7.3E-03	5.1E-03	8.0E-04	2.3E-04	0.11	0.003	**
A_0033	XA0005	1.2E-03	1.5E-04	1.2E-04	2.5E-05	0.10	1.4E-09	***
C_0042	*N*-Methylproline	2.6E-03	2.5E-03	2.6E-04	1.7E-04	0.10	0.074	
A_0045	*cis*-Aconitic acid	3.2E-02	1.1E-02	7.1E-04	2.8E-04	0.02	1.3E-05	***
A_0057	Citric acid	2.6E+00	2.1E-01	1.3E-02	3.0E-03	0.005	2.2E-11	***
C_0056	Adenine	6.3E-02	5.9E-03	N.D.	N.A.	<1	N.A.	
C_0113	XC0044	2.1E-04	4.3E-05	N.D.	N.A.	<1	N.A.	
C_0134	Gly-His	1.0E-04	1.8E-05	N.D.	N.A.	<1	N.A.	
	His-Gly							
C_0181	XC0135	7.1E-05	4.7E-05	N.D.	N.A.	<1	N.A.	

'C' and 'A' in ID denote cation and anion modes respectively

'N.D - Not Detected. The target peak or metabolite was below detection limits;

'N.A. - Not available. Calculation was not possible because of insufficient data.

'"Control" refers to uninfected inidividuals; "Disease" refers to O. volvulus infected individuals

'Mean - Average of all samples in the group; S.D. - Standard deviation

'Relative Area - Calculated as the ratio of metabolite peak area to the internal standard peak area

[¶] - The ratio of averaged detection values

[#] - p-value determined by Welch's t-test (

*<0.05,

**<0.01,

***<0.001)

Table 3

Known-unknowns

Peak ID	Mode	Mass	Formula	KEGG Database	HMDB database
XC0001	Cation	71.073	C4H9N	C12244	
XC0016	Cation	128.058	C5H8N2O2	C00906,C05717,C05715	HMDB00079
XC0017	Cation	129.089	C5H11N3O	C02647	
XC0029	Cation	143.094	C7H13NO2	C10172	HMDB04827
XC0040	Cation	173.079	C6H11N3O3	C03771	HMDB04225
XC0061	Cation	217.13	C10H19NO4	C03017	HMDB00824
XC0065	Cation	220.083	C11H12N2O3	C00643,C01017,C09985	HMDB00472
XC0071	Cation	233.172	C10H23N3O3	HMDB11140	
XC0089	Cation	254.089	C11H14N2O5	C16582,C16584	
XC0120	Cation	297.044	C8H15N3O5S2	HMDB00709	
XC0126	Cation	309.104	C11H19NO9	C00270,C03525	HMDB00773,HMDB00230
XC0132	Cation	324.152	C12H24N2O8	HMDB00600	
XC0137	Cation	349.093	C12H19N3O7S	C14871	
XA0002	Anion	111.993	CH5O4P	C06455	
XA0003	Anion	125.999	C2H6O4S	C05123	HMDB03903
XA0004	Anion	145.038	C5H7NO4	C00940,C05572	HMDB01552
XA0012	Anion	167.025	C4H9NO4S	HMDB06462	
XA0013	Anion	173.999	C6H6O4S	C00850,C02180,C12849	
XA0017	Anion	187.121	C9H17NO3	C12029,C01092	
XA0019	Anion	192.027	C6H8O7	C00451,C04617,C04575	HMDB06511,HMDB00094
				C02780,C03921,C00679	HMDB05971,HMDB00193
				C03600,C00158,C00311	HMDB01874
XA0027	Anion	228.208	C14H28O2	C06424	HMDB02221,HMDB00806
XA0033	Anion	243.087	C9H13N3O5	C00475,C02961,C05711	HMDB00089
XA0035	Anion	255.988	C6H8O9S	C02812	
XA0036	Anion	255.988	C6H8O9S	C02812	
XA0055	Anion	370.006	C7H16O13P2	C00447,C11472	

Peak ID	Mode	Mass	Formula	KEGG Database	HMDB database
XA0065	Anion	446.06	C11H20N4O11P2	C00570	HMDB01564

Table 4

Quantification of Metabolites

ID	Metabolite	Control		Disease		Comparative Analysis		
						Disease vs Control		
		Mean	S.D.	Mean	S.D.	Ratio ¶	*p*-value ‖	
A_0001	Glyoxylic acid	N.D.	N.A.	N.D.	N.A.	N.A.	N.A.	
A_0002	Glycolic acid	N.D.	N.A.	N.D.	N.A.	N.A.	N.A.	
A_0003	Pyruvic acid	113	43	161	54	1.4	0.069	
A_0005	Lactic acid	2,446	792	5,587	3,453	2.3	0.019	*
A_0007	2-Hydroxybutyric acid	41	13	25	10	0.6	0.007	**
A_0008	3-Hydroxybutyric acid	75	90	27	17	0.4	0.136	
A_0011	Fumaric acid	N.D.	N.A.	N.D.	N.A.	N.A.	N.A.	
A_0012	2-Oxoisovaleric acid	14	3.7	12	3.2	0.9	0.254	
A_0015	Succinic acid	14	3.3	11	3.3	0.8	0.060	
A_0027	Malic acid	12	5.3	15	6.2	1.3	0.222	
A_0032	2-Oxoglutaric acid	36	20	16	8.7	0.5	0.022	*
A_0038	Phosphoenolpyruvic acid	N.D.	N.A.	N.D.	N.A.	N.A.	N.A.	
A_0040	Glyceraldehyde 3-phosphate	N.D.	N.A.	N.D.	N.A.	N.A.	N.A.	
A_0041	Dihydroxyacetone phosphate	N.D.	N.A.	N.D.	N.A.	N.A.	N.A.	
A_0043	Glycerol 3-phosphate	9.7	5.3	2.3	1.6	0.2	0.009	**
A_0045	*cis*-Aconitic acid	220	79	5.0	2.0	0.02	1.3E-05	***
A_0050	2-Phosphoglyceric acid	N.D.	N.A.	N.D.	N.A.	N.A.	N.A.	
A_0051	3-Phosphoglyceric acid	N.D.	N.A.	N.D.	N.A.	N.A.	N.A.	
A_0056	Isocitric acid	63	44	6.9	2.0	0.11	0.003	**
A_0057	Citric acid	24,230	1,943	120	28	0.005	2.2E-11	***
A_0059	Gluconic acid	8.0	2.1	5.4	1.3	0.7	0.005	**
A_0060	Erythrose 4-phosphate	N.D.	N.A.	N.D.	N.A.	N.A.	N.A.	
A_0075	Ribulose 5-phosphate	N.D.	N.A.	2.2	N.A.	1<	N.A.	
A_0076	Ribose 5-phosphate	N.D.	N.A.	N.D.	N.A.	N.A.	N.A.	

ID	Metabolite	Control		Disease		Comparative Analysis	
						Disease vs Control	
		Mean	S.D.	Mean	S.D.	Ratio ¶	*p*-value ‖
A_0092	Glucose 6-phosphate	2.6	1.4	3.7	N.A.	1.4	N.A.
A_0093	Glucose 1-phosphate	N.D.	N.A.	N.D.	N.A.	N.A.	N.A.
A_0094	Fructose 6-phosphate	N.D.	N.A.	N.D.	N.A.	N.A.	N.A.
A_0100	6-Phosphogluconic acid	N.D.	N.A.	N.D.	N.A.	N.A.	N.A.
A_0105	Sedoheptulose 7-phosphate	N.D.	N.A.	N.D.	N.A.	N.A.	N.A.
A_0113	dTMP	N.D.	N.A.	N.D.	N.A.	N.A.	N.A.
A_0114	CMP	N.D.	N.A.	N.D.	N.A.	N.A.	N.A.
A_0115	UMP	N.D.	N.A.	N.D.	N.A.	N.A.	N.A.
A_0118	cAMP	N.D.	N.A.	N.D.	N.A.	N.A.	N.A.
A_0121	Fructose 1,6-diphosphate	N.D.	N.A.	N.D.	N.A.	N.A.	N.A.
A_0125	cGMP	N.D.	N.A.	N.D.	N.A.	N.A.	N.A.
A_0126	AMP	N.D.	N.A.	N.D.	N.A.	N.A.	N.A.
A_0127	IMP	N.D.	N.A.	N.D.	N.A.	N.A.	N.A.
A_0131	GMP	N.D.	N.A.	N.D.	N.A.	N.A.	N.A.
A_0135	CoA_divalent	N.D.	N.A.	N.D.	N.A.	N.A.	N.A.
A_0137	PRPP	N.D.	N.A.	N.D.	N.A.	N.A.	N.A.
A_0139	dTDP	N.D.	N.A.	N.D.	N.A.	N.A.	N.A.
A_0140	CDP	N.D.	N.A.	N.D.	N.A.	N.A.	N.A.
A_0141	UDP	N.D.	N.A.	N.D.	N.A.	N.A.	N.A.
A_0142	Acetyl CoA_divalent	N.D.	N.A.	N.D.	N.A.	N.A.	N.A.
A_0143	Malonyl CoA_divalent	N.D.	N.A.	N.D.	N.A.	N.A.	N.A.
A_0144	ADP	N.D.	N.A.	N.D.	N.A.	N.A.	N.A.
A_0145	GDP	N.D.	N.A.	N.D.	N.A.	N.A.	N.A.
A_0147	dCTP	N.D.	N.A.	N.D.	N.A.	N.A.	N.A.
A_0148	dTTP	N.D.	N.A.	N.D.	N.A.	N.A.	N.A.
A_0149	CTP	N.D.	N.A.	N.D.	N.A.	N.A.	N.A.
A_0150	UTP	N.D.	N.A.	N.D.	N.A.	N.A.	N.A.

ID	Metabolite	Control		Disease		Comparative Analysis		
						Disease vs Control		
		Mean	S.D.	Mean	S.D.	Ratio ¶	*p*-value ‖	
A_0151	dATP	N.D.	N.A.	N.D.	N.A.	N.A.	N.A.	
A_0153	ATP	N.D.	N.A.	N.D.	N.A.	N.A.	N.A.	
A_0154	GTP	N.D.	N.A.	N.D.	N.A.	N.A.	N.A.	
A_0156	NAD^+	N.D.	N.A.	N.D.	N.A.	N.A.	N.A.	
A_0158	$NADP^+$	N.D.	N.A.	N.D.	N.A.	N.A.	N.A.	
C_0004	Gly	297	136	343	115	1.2	0.420	
C_0009	Putrescine	N.D.	N.A.	N.D.	N.A.	N.A.	N.A.	
C_0010	Sarcosine	1.7	0.6	1.6	0.5	0.9	0.680	
C_0011	Ala	430	103	377	111	0.9	0.280	
C_0012	β-Ala	3.0	2.2	2.4	0.7	0.8	0.448	
C_0015	GABA	0.3	0.04	0.4	0.3	1.5	0.399	
C_0016	*N,N*-Dimethylglycine	3.0	0.8	3.9	1.0	1.3	0.041	*
C_0019	Choline	68	21	25	8.2	0.4	5.0E-05	***
C_0020	Ser	127	48	113	50	0.9	0.549	
C_0022	Cytosine	N.D.	N.A.	N.D.	N.A.	N.A.	N.A.	
C_0024	Uracil	N.D.	N.A.	N.D.	N.A.	N.A.	N.A.	
C_0025	Creatinine	70	24	52	20	0.7	0.087	
C_0026	Pro	235	52	173	42	0.7	0.010	**
C_0030	Val	245	54	163	46	0.7	0.002	**
C_0031	Betaine	60	17	46	13	0.8	0.058	
C_0033	Thr	167	45	100	32	0.6	0.002	**
C_0034	Homoserine	N.D.	N.A.	0.2	N.A.	1<	N.A.	
C_0035	Betaine aldehyde_+H_2O	N.D.	N.A.	N.D.	N.A.	N.A.	N.A.	
C_0036	Cys	N.D.	N.A.	N.D.	N.A.	N.A.	N.A.	
C_0039	Thymine	N.D.	N.A.	N.D.	N.A.	N.A.	N.A.	
C_0045	Hydroxyproline	13	8.3	13	5.6	1.0	0.986	
C_0046	Creatine	37	18	38	32	1.0	0.928	

ID	Metabolite	Control		Disease		Comparative Analysis		
						Disease vs Control		
		Mean	S.D.	Mean	S.D.	Ratio ¶	*p*-value ‖	
C_0047	Leu	116	34	85	37	0.7	0.067	
C_0048	Ile	70	24	42	20	0.6	0.010	*
C_0050	Asn	33	8.8	48	22	1.5	0.065	
C_0052	Ornithine	67	21	66	40	1.0	0.924	
C_0053	Asp	16	5.2	10	13	0.6	0.216	
C_0056	Adenine	205	19	N.D.	N.A.	<1	N.A.	
C_0057	Hypoxanthine	3.5	1.1	9.2	2.9	2.6	9.3E-05	***
C_0059	Anthranilic acid	N.D.	N.A.	N.D.	N.A.	N.A.	N.A.	
C_0061	Tyramine	N.D.	N.A.	N.D.	N.A.	N.A.	N.A.	
C_0074	Spermidine	N.D.	N.A.	N.D.	N.A.	N.A.	N.A.	
C_0075	Gln	386	105	460	126	1.2	0.177	
C_0077	Lys	224	52	162	45	0.7	0.011	*
C_0078	Glu	263	82	99	98	0.4	7.6E-04	***
C_0081	Met	17	5.1	19	15	1.1	0.758	
C_0085	Guanine	0.5	0.5	0.14	0.06	0.3	0.476	
C_0088	His	97	17	75	21	0.8	0.016	*
C_0099	Phe	70	14	54	25	0.8	0.104	
C_0105	Arg	112	31	50	26	0.5	1.4E-04	***
C_0107	Citrulline	33	12	25	8.2	0.8	0.100	
C_0110	Tyr	80	17	46	19	0.6	5.2E-04	***
C_0125	Spermine	N.D.	N.A.	N.D.	N.A.	N.A.	N.A.	
C_0129	Trp	50	8.6	26	11	0.5	5.6E-05	***
C_0141	Carnosine	N.D.	N.A.	N.D.	N.A.	N.A.	N.A.	
C_0149	Thymidine	N.D.	N.A.	N.D.	N.A.	N.A.	N.A.	
C_0151	Cytidine	N.D.	N.A.	N.D.	N.A.	N.A.	N.A.	
C_0152	Uridine	12	1.7	14	3.0	1.1	0.123	
C_0162	Adenosine	N.D.	N.A.	N.D.	N.A.	N.A.	N.A.	

ID	Metabolite	Control		Disease		Comparative Analysis		
						Disease vs Control		
		Mean	S.D.	Mean	S.D.	Ratio ¶	*p*-value ‖	
C_0163	Inosine	N.D.	N.A.	2.3	1.6	1<	N.A.	
C_0168	Guanosine	N.D.	N.A.	0.4	0.3	1<	N.A.	
C_0175	Glutathione (GSSG)_divalent	N.D.	N.A.	0.3	0.15	1<	N.A.	
C_0176	Glutathione (GSH)	N.D.	N.A.	N.D.	N.A.	N.A.	N.A.	
C_0184	S-Adenosylmethionine	N.D.	N.A.	N.D.	N.A.	N.A.	N.A.	

‘C’ and ‘A’ in ID denote cation and anion modes respectively
‘N.D - Not Detected. The target peak or metabolite was below detection limits;
‘N.A. - Not available. Calculation was not possible because of insufficient data.
‘‘“Control” refers to uninfected inidividuals; “Disease” refers to O. volvulus infected individuals
‘Mean - Average of all samples in the group; S.D. - Standard deviation; Values denote concentrations in mM.

¶ - The ratio of averaged detection values

- p-value determined by Welch’s t-test (

* <0.05,

** <0.01,

*** <0.001)